ACS APPLIED MATERIALS & INTERFACES

Research Article

www.acsami.org

Iron Oxide@PEDOT-Based Recyclable Photothermal Nanoparticles with Poly(vinylpyrrolidone) Sulfobetaines for Rapid and Effective Antibacterial Activity

Chan Jin Jeong,[†] Shazid Md. Sharker,[‡] Insik In,*[,†,§] and Sung Young Park*[,†,∥]

[†]Department of IT Convergence, [§]Department of Polymer Science and Engineering, and [∥]Department of Chemical and Biological Engineering, Korea National University of Transportation, Chungju 380-702, Republic of Korea

[‡]Department of Chemistry, KAIST, Daejeon 305-701, Republic of Korea

Supporting Information

ABSTRACT: Growing microbial resistance that renders antibiotic treatment vulnerable has emerged, attracting a great deal of interest in the need to develop alternative antimicrobial treatments. To contribute to this effort, we report magnetic iron oxide (Fe_3O_4) nanoparticles (NPs) coated with catechol-conjugated poly(vinylpyrrolidone) sulfobetaines (C-PVPS). This negatively charged Fe_3O_4@C-PVPS is subsequently encapsulated by poly(3,4-ethylenedioxythiophene) (PEDOT) following a layer-by-layer (LBL) self-assembly method. The obtained Fe_3O_4@C-PVPS:PEDOT nanoparticles appear to be novel NIR-irradiated photothermal agents that can achieve effective bacterial killing and are reusable after isolation of the used particles using external magnetic fields. The recyclable Fe_3O_4@C-PVPS:PEDOT NPs exhibit a high efficiency in converting photothermal heat for rapid antibacterial effects against *Staphylococcus aureus* and *Escherichia coli*. In this study, antibacterial tests for repeated uses maintained almost 100% antibacterial efficiency during three cycles and provided rapid and effective killing of 99% Gram-positive and -negative bacteria within 5 min of near-infrared (NIR) light exposure. The core−shell nanoparticles (Fe_3O_4@C-PVPS:PEDOT) exhibit the required stability, and their paramagnetic nature means that they rapidly convert photothermal heat sufficient for use as NIR-irradiated antibacterial photothermal sterilizing agents.

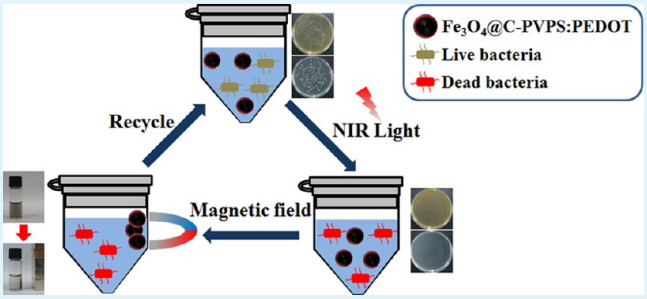

KEYWORDS: *iron oxide, PEDOT, near-infrared, antibacterial activity, recyclable, photothermal*

INTRODUCTION

The frequent and excessive use of conventional antibiotics and the habitual tendency of microbial strains to grow resistant are becoming global concerns.[1] Innovative materials and environmentally friendly methods to address this threat and completely eradicate microbial resistance are therefore parallel strategies with traditional antibiotics.[2] In this effort, different nanomaterial-based antibacterial agents have shown promise.[3] The properties of the bacterial cell wall play a crucial role in the diffusion of therapeutic agents inside biofilm matrixes, and this biofilm formation protects pathogenic bacteria against antibiotics and slow-growing bacteria that are related to the expression of stress-response genes responsible for microbial resistance. However, nanomaterials have high surface area-to-volume ratios, resulting in the appearance of new mechanical, chemical, electrical, optical, magnetic, and electro-optical properties enabling them to attach to and disrupt the integrity of the bacterial membrane. This results in the increasing uptake and bioaccumulation of nanoparticles on biofilms to fight against microbial resistance.[4] The most popular agents are gold (Au) and silver (Ag) nanoparticles (NPs), although researchers have shown specific interest in graphene oxide (GO) and some interest in functionalized iron oxide (Fe_3O_4) nanoparticles for use as antibacterial nanomaterials.[5−10] Although most of these materials have shown interesting results, many have been developed for only a single or one-time use. The very small quantities of nanomaterials in these applications do not warrant their consideration as an environmental hazard, and such single applications limit their vast potential, although immense interest has been shown in their use as environmentally friendly antibacterial nanomaterials.[2] However, extensive use of nanoparticles (NPs) in biological science, medical science, and commercial products might lead to the leakage and accumulation of NPs in the environment (soil, water, etc.). Protection of the environment and beneficial bacteria from NPs is needed for the development of reusable and recyclable NPs.[4]

Related to the material development, poly(vinylpyrrolidone)s (PVPs) are widely used to synthesize colloidal particles as capping and stabilizing agents. The capping particles are formed from a complex interlayer with another ligand through

Received: January 12, 2015
Accepted: April 23, 2015
Published: April 23, 2015

DOI: 10.1021/acsami.5b02737
ACS Appl. Mater. Interfaces 2015, 7, 9469−9478

hydrogen bonding and can be further fabricated to develop low-pH-sensitive drug-delivery systems.[11] Recently, functionalized magnetic nanoparticles have shown great capability for detecting and capturing bacteria at very high concentrations. An immobilized target sample on the surface of magnetic nanoparticles promises to improve detection and isolation as a result of magnetized stimulus control through an external magnet.[12] Moreover, the ability to disperse functionalized magnetic nanoparticles in a sample mixture enables rapid contact between the particles and their ligand sample that would ultimately result in lower limits of detection and shorter analysis times.[2] For the development of conducting materials, poly(3,4-ethylenedioxythiophene) (PEDOT) is easily processed, relatively simple to produce at low cost, transparent, stable against oxidation, and highly susceptible to the absorption of ultraviolet (UV), visible (vis), and near-infrared (NIR) light.[13,14] In addition, the incorporation of a water-soluble polyelectrolyte, such as sultone with PEDOT, increases the water solubility, film-forming properties, and native conduction efficiency.[15] However, the advantages of using adhesive catechol on immobilized sultone-modified PEDOT on an inorganic nanoparticle surface to take full advantage of these beneficial opportunities are still little researched.[16]

NIR-absorbing nanoparticles have proven to be prominent tools for photothermal cancer treatment. Recently, NIR-irradiated nanoparticles using photothermolysis of the microbial strain have attracted considerable interest for the development of renewable antibiotic nanomaterials.[11] Furthermore, the increased level of resistance to traditional antibiotics has also motivated the consideration of these new types of antibacterial methods. NIR irradiation itself has no effect on microbial strains; however, when phototargeting nanoparticles are able to absorb light with wavelengths of 750−950 nm (NIR region), the photoenergy is converted into thermal energy, sufficient to kill living cells.[15] Therefore, NIR-sensitive silver-deposited polymeric iron oxide (Ag−Fe_3O_4), graphene−Fe_3O_4, graphene oxide−Ag nanoparticles, quaternary-amine-conjugated Fe_3O_4, polyethylenimine-combined graphene oxide−Ag hybrid materials, and gold nanoparticles (AuNPs), in conjunction with mainstream antibiotics treatment, have attracted significant attention.[5−10] Despite those interesting findings, the use of NIR responsive functionalize Fe_3O_4-based nanoparticles that can photothermally kill bacteria in a recyclable and synergistic way remain to be further explored. However, when the typical antibiotic treatment fails to fight bacteria of a resistant strain, NIR-irradiated nanomaterials can be used rather than the traditional antibiotic treatment. Recyclable photothermal nanomaterials offer multiple applicable requirements for conventional antibiotics.

In this work, we report NIR-light-absorbing recyclable iron oxide-functionalized nanoparticles for the rapid and effective killing of Gram-positive and Gram-negative bacteria. To achieve this goal, iron oxide nanoparticles (Fe_3O_4) were coated with catechol-conjugated poly(vinylpyrrolidone) sulfobetaine (C-PVPS) by mussel-inspired adhesion on the surface of Fe_3O_4 to acquire a negative charge (C-PVPS-coated Fe_3O_4). The Fe_3O_4@C-PVPS was additionally assembled with poly(3,4-ethylenedioxythiophene) (PEDOT) to provide sustained stability and ensure that the overall scheme was recyclable and capable of absorbing NIR light while capturing the surrounding bacteria, which can subsequently release sufficient photothermal heat. Therefore, our study presents a multifunctional iron oxide nanoparticle (Fe_3O_4@C-PVPS:PEDOT) as an effective NIR-irradiated recyclable antibacterial sterilizing agent.

EXPERIMENTAL SECTION

Materials. Iron oxide(II, III) nanopowder less than 50 nm (Fe_3O_4), poly(vinylpyrrolidone) (PVP, Mw 55,000), 2-chloro-3′,4′-hydroxyacetophenone (CCDP), 3,4-ethylenedioxythiophene (EDOT), 1,3-propane sultone, iron(III) sulfate hydrate, ethanol, tetrahydrofuran (THF), HCl, trizma base (99%, Sigma), trizma HCl, (99%, Sigma), diethyl ether, hexane, deuterium oxide (D_2O), de Man−Rogosa−Sharpe (MRS) broth, Luria−Bertani (LB) broth, phosphate-buffered saline (PBS) solution, and agar powder were purchased from Sigma-Aldrich, Seoul, Korea.

Synthesis of Catechol-Conjugated Poly(vinylpyrrolidone) Sulfobetaine (C-PVPS). Catechol- and sultone-quaternized PVP was synthesized following a method similar to that in refs 16 and 17. Specifically, 0.18 mmol of catechol-quaternized PVP (C-PVP, MW 60030) and 1,3-propane sultone (0.046 mol) were dissolved in 100 mL of anhydrous ethanol and THF in a 250 mL flask. The mixture was stirred for 12 h at 35 °C under a nitrogen atmosphere. After stirring, the solvent was evaporated in a rotary evaporator, and the mixture was precipitated using cold diethyl ether. The yield of the C-PVPS was 72% of the initial given amount of reactants. The degree of quaternization was estimated to be 30 catechol and 130 sulfobetaine units per PVP chain.

^{1}H NMR (400 MHz, D_2O, δ): 1.77−2.0 (2H, —CH_2— of PVP), 2.12−2.23 (2H, —CH_2— of VP ring), 2.24−2.32 (2H, —CH_2— of VP ring), 2.9−3.0 (2H, —CH_2—SO_3— of sultone), 3.15−3.28 (2H, —CH_2— of VP ring), 3.47−3.66 (H, —CH— of PVP), 6.67−7.53 (aromatic protons of catechol).

Preparation of C-PVPS-Coated Fe_3O_4 (Fe_3O_4@C-PVPS). Fe_3O_4 nanoparticles (50 mg) were dispersed in 5 mL of THF, and this solution was added dropwise to 500 mg of C-PVPS that was initially dissolved in 30 mL of ethanol. The resulting mixture was then stirred for 24 h at room temperature. After the end of the reaction time, the solvent was evaporated in a rotary evaporator, and the mixture was precipitated using hexane. The sample was then centrifuged to obtain a dark pellet of nanoparticles. After the hexane had been filtered, the Fe_3O_4@C-PVPS was readily dispersed in water. The Fe_3O_4@C-PVPS was then filtered and freeze-dried.

Synthesis of Fe_3O_4@C-PVPS:PEDOT. Fe_3O_4@C-PVPS (20 mg), iron(II) sulfate hydrate (200 mg), and EDOT (2000 mg) were dissolved in 80 mL of deionized water (pH 8−9) in a 250 mL flask. The mixture was stirred for 48 h at 50 °C under a nitrogen atmosphere.[16] After the reaction time, the solvent was washed in a centrifuge and precipitated three times using deionized water and THF. The product (Fe_3O_4@C-PVPS:PEDOT) was then filtered and freeze-dried. To evaluate the photothermal efficiency, we synthesized Fe_3O_4@C-PVPS:PEDOT (1:10) and Fe_3O_4@C-PVPS:PEDOT (1:100) differing only in the EDOT dissolution ratio.

Characterization. C-PVPS was determined by ^{1}H NMR spectroscopy (Bruker AVANCE 400 spectrometer operating at 400 MHz) using D_2O as the solvent. UV−vis−NIR absorption spectra were obtained on an Optizen 2120 UV spectrophotometer (Mecasys Co. Ltd.). Field-emission scanning electron microscopy (FE-SEM) micrographs and energy-dispersive X-ray (EDX) spectra were obtained with a JSM-6700 (GELO) instrument. For SEM analysis, powder samples were prepared. Transmission electron microscopy (TEM) images were investigated using a Technai F-20 FE-TEM instrument (FEI, Eindhoven, The Netherlands) at 200 kV. Particle size was measured by dynamic laser light scattering (Zetasizer Nano, Malvern Instruments GmbH, Herrenberg, Germany). X-ray photoelectron spectroscopy (XPS) spectra were obtained to measure the surface atomic composition using an ESCALAB apparatus (Omicrometer, Taunusstein, Germany). The magnetic properties of the prepared samples were measured with an alternating gradient magnetometer (AGM; 2900-02 AGIM, PMC Co.). The distance between the NIR diode laser and the bacteria solution was 5 cm, the irradiation area was 2 cm^2, and

DOI: 10.1021/acsami.5b02737
ACS Appl. Mater. Interfaces 2015, 7, 9469−9478

Scheme 1. (a) Illustration of the Synthesis Routes of Fe_3O_4@C-PVPS:PEDOT and (b) Schematic Representation of NIR-Irradiated Antibacterial Activity Followed by Application of a Magnetic Field to Isolate and Recycle Fe_3O_4@C-PVPS:PEDOT

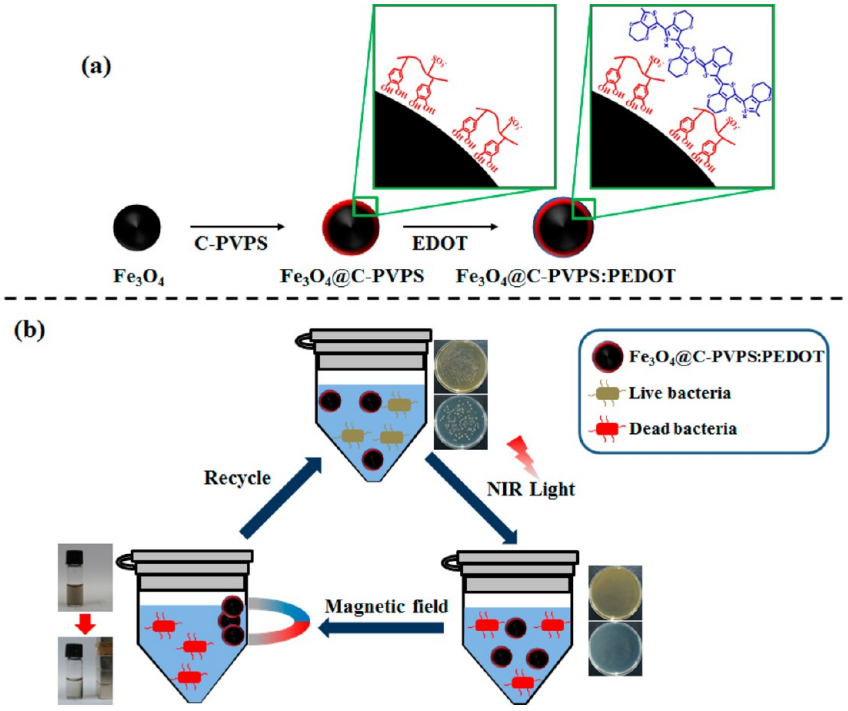

the solution volume was 0.2 mL. Thermogravimetric analysis (TGA) was performed on a TGA-DSC1 system (Star; Mettler-Toledo).

Photothermal Effect of Fe_3O_4@C-PVPS:PEDOT. An optical-fiber-coupled 808-nm high-power diode laser (PSU-III-LRD, CNI Optoelectronics Technology Co. Ltd., Changchun, China) was used to irradiate bacteria during our experiments. For photothermal treatment, a laser beam with a diameter of 10 mm was focused on the bacteria solution at a power density of 2 W/cm^2 for 5 min. Infrared thermal images were taken with an NEC Avio Thermo Tracer TH9100 thermal imaging camera.

Antibacterial Activity after NIR Exposure of Fe_3O_4@C-PVPS:PEDOT. The photothermal antibacterial activities of the Fe_3O_4@C-PVPS:PEDOT materials were examined against *Staphylococcus aureus* (*S. aureus*) and *Escherichia coli* (*E. coli*) by the following methods: Stock solutions of *Staphylococcus aureus* (Gram-positive, strain ATCC 25424) and *E. coli* (Gram-negative, strain ATCC 25922) were prepared in LB broth and MRS broth (50 mL). After incubation at 37 °C for 12 h, the bacterial content of the suspension was 10^8 cells. The suspension dilution was 10^5 cells using a peptone solution. As a corollary, in a Petri dish, a single layer of solid medium was created upon which the bacterial suspension was poured. The antibacterial activity of Fe_3O_4@C-PVPS:PEDOT was determined against the Gram-positive bacteria *S. aureus* and Gram-negative bacteria *E. coli* through a viable-cell-colony counting method. Colonies of *S. aureus* and *E. coli* grown on MRS and LB plates were used to inoculate 10 mL of MRS broth and 10 mL of LB nutrient broth, respectively, and the mixtures were incubated at 37 °C overnight under shaking at 150 rpm (Lab Companion SI-600R benchtop shaker). Overnight cultures were measured by UV−vis spectroscopy at 600 nm with absorbance adjusted to 0.6 to confirm the turbidity standard according to the McFarland scale. At this stage, the cultures contained ca. ~10^8 cells/mL. Then, the microorganism suspensions were diluted, and 10 μL of both bacteria [5×10^5 colony-forming units (CFU)/mL] were placed in 1 mL of nutrient broth with various concentration of Fe_3O_4@C-PVPS:PEDOT and irradiated with 808-nm laser light at a power density of 2 W/m^2 for 5 min. Then, 0.1 mL of the suspension was collected, diluted, and spread on an agar plate at different time intervals. Each dilution had three parallel groups. After being rubbed for 2 min, the substances were incubated at 37 °C for 24 h, and the bacterial colonies were inspected.

Recycling of Fe_3O_4@C-PVPS:PEDOT for Antibacterial Tests. Fe_3O_4@C-PVPS:PEDOT was incubated with 1 mL of cell suspension of both *S. aureus* and *E. coli* (10^5−10^6) in a 2 mL eppendorf (EP) tube at 2 W/m^2 for 5 min (808-nm laser). Afterward, the tube was placed in a magnetic separation stand at room temperature for 3 min. The nanoparticles were attracted to the wall of the tube by a magnetic force. After the supernatant had been removed from the tube, 0.1 mL of the supernatant was diluted appropriately and plated onto solid MRS and LB agar plates. Each viable bacterium formed into a bacterial colony that was counted after being incubated at 37 °C for 24 h. The recycled magnetite nanoparticles were incubated with a fresh sample of 5 mL of cell suspension in the EP conical tube at 2 W/m^2 for 5 min (808-nm laser). The methods described above were repeated according to the same procedures three more times. In each cycle, the magnetic nanoparticles were collected only by exposure to an external magnetic field without washing with PBS buffer solution.

Fluorescence Microscopy. For fluorescence cell imaging, 1 mL of bacterial suspension containing 10^5 CFU/mL was centrifuged (4000 rpm for 5 min) and resuspended in 50 μL of PBS. Then, 5 μL of the bacterial suspension was combined with 20 μL of a fluorescent probe mixture containing 3.0 μM green fluorescent nucleic acid stain SYTO 9 (Invitrogen, Carlsbad, CA) and 15.0 μM red fluorescent nucleic acid stain PI (Sigma-Aldrich, St. Louis, MO). Fe_3O_4@C-PVPS:PEDOT was incubated with 1 mL of bacterial suspension of both *S. aureus* and *E. coli* (10^5−10^6) in a 2 mL EP tube at 2 W/m^2 for 5 min (808-nm laser). The mixture was incubated in the dark for 15 min, and a 5 μL aliquot was placed on a glass slide, which was then covered with a coverslip, sealed, and examined under an LSM510 confocal laser scanning microscope (Carl Zeiss, Oberkochen, Germany) with a 364-nm UV laser excited by a 543-nm HeNe laser.

RESULTS AND DISCUSSION

To prepare recyclable antimicrobial PTT agents, we developed a very simple procedure to make functionalized Fe_3O_4 coated with a robust adhesive material containing a catechol moiety conjugated with poly(vinylpyrrolidone). Finally, the Fe_3O_4@C-

DOI: 10.1021/acsami.5b02737
ACS Appl. Mater. Interfaces 2015, 7, 9469−9478

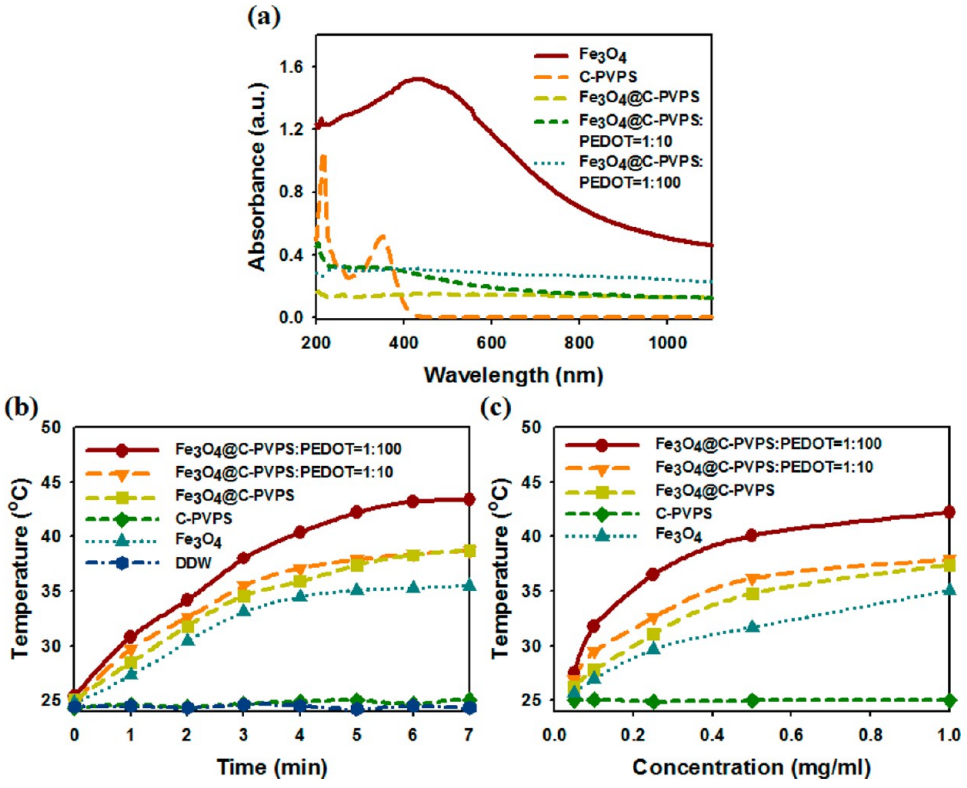

Figure 1. (a) UV−visible−NIR absorption spectra of Fe_3O_4, C-PVPS, Fe_3O_4@C-PVPS, and Fe_3O_4@C-PVPS:PEDOT (1:10 and 1:100 in water; 0.1 mg/mL, total content). (b) Photothermal heat generation curves of pure water, Fe_3O_4, C-PVPS, Fe_3O_4@C-PVPS, and Fe_3O_4@C-PVPS:PEDOT (1:10 and 1:100; 1 mg/mL concentration) under 808-nm laser irradiation with a power density of 2 W/cm^2. (c) Concentration-dependent photothermal elevation curve of panel b.

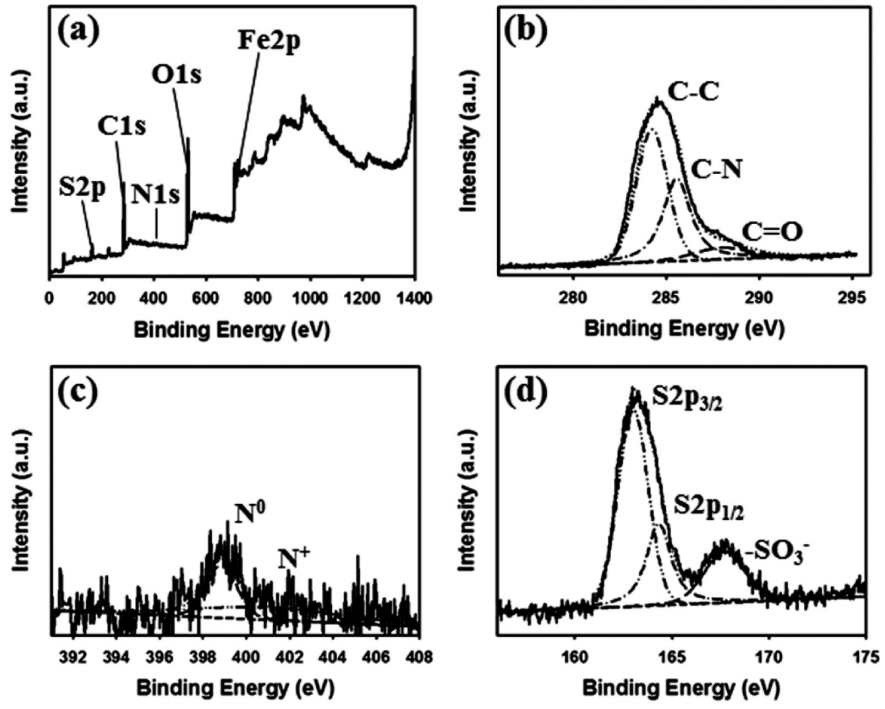

Figure 2. XPS spectra of Fe_3O_4@C-PVPS:PEDOT (1:100): (a) survey scan and (b−d) narrow-scale scans of (b) C 1s, (c) N 1s, and (d) S 2p peaks.

PVPS particles were coated with PEDOT-like encapsulation (Fe_3O_4@C-PVPS:PEDOT) as depicted in Scheme 1.[16,18] The catechol-conjugated PVPS with PEDOT facilitated the stable encapsulation of Fe_3O_4 nanoparticles with PEDOT retained on the outer surface for NIR absorption. This scheme maintained required the stability and resulted in recyclable intact nanoparticles after photothermal heating, and finally provided sustain antibacterial activity for multiple applications.

DOI: 10.1021/acsami.5b02737
ACS Appl. Mater. Interfaces 2015, 7, 9469−9478

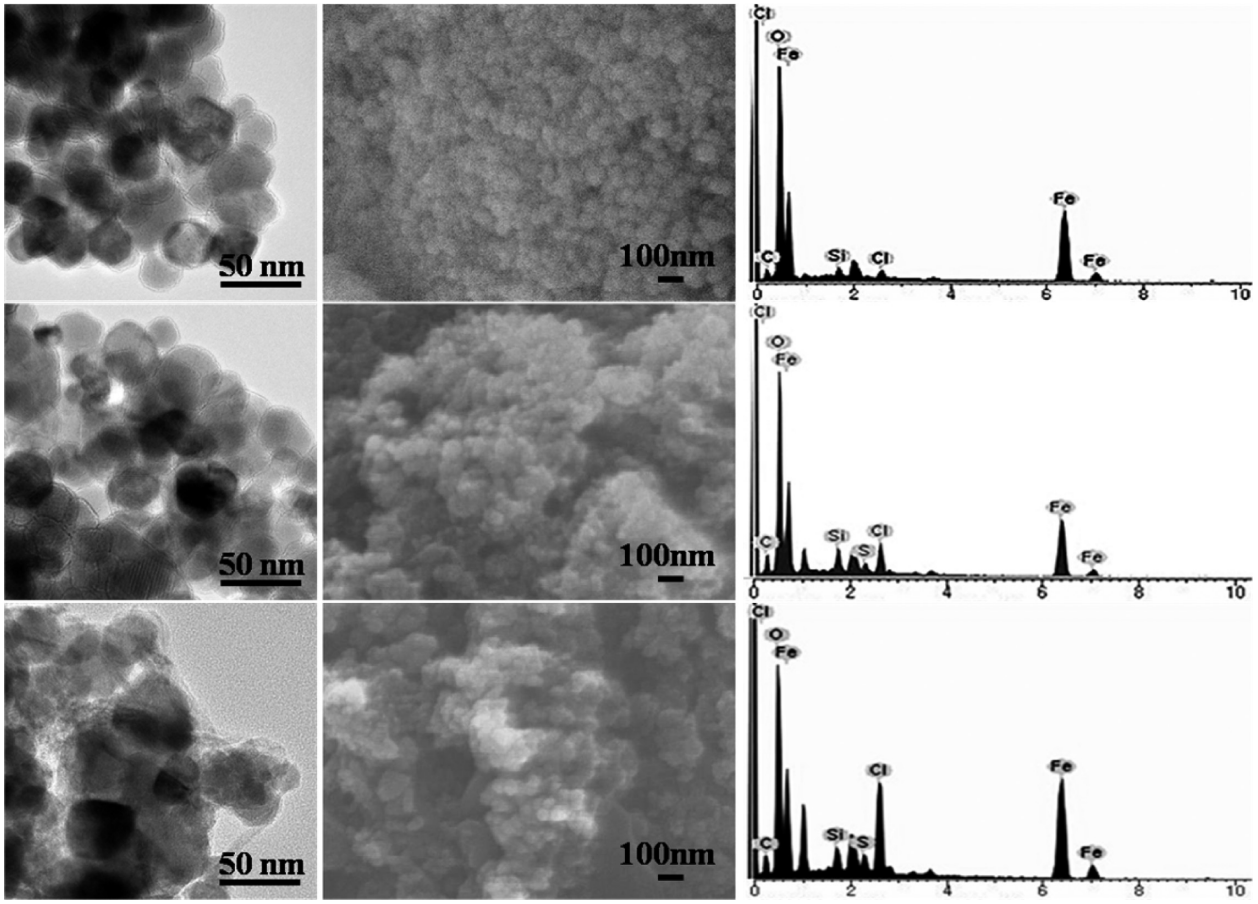

Figure 3. TEM image, SEM images and EDX spectra of (top) Fe_3O_4@C-PVPS, (middle) Fe_3O_4@C-PVPS:PEDOT (1:10), and (bottom) Fe_3O_4@C-PVPS:PEDOT (1:100).

The UV−vis−NIR absorbance spectra of Fe_3O_4, C-PVPS, Fe_3O_4@C-PVPS, and Fe_3O_4@C-PVPS:PEDOT exhibited an increased absorption band from the visible to the NIR region with increasing of PEDOT amounts for Fe_3O_4@C-PVPS:PEDOT (Figure 1a). However, instead of sharp peaks, the Fe_3O_4@C-PVPS and Fe_3O_4@C-PVPS:PEDOT materials maintained broad optical absorption bands in the UV−vis−NIR region from 0 to 5 days without any noticeable changes, which was comparable to the behavior reported elsewhere [Figures S1 and S2, Supporting Information (SI)].[18]

NIR-irradiated photothermal therapy (PTT) is a widely used treatment strategy for the thermolysis of pathogenic cells. Recently, poly(3,4-ethylenedioxythiophene: poly(styrenesulfonate) (PEDOT:PSS) composites were reported to be capable of the hyperthermic destruction of multiple-drug-resistant bacteria (MDRB). This achievement has thus attracted considerable interest in antibacterial treatment.[4] The NIR-laser-mediated temperature elevation profile (Figure 1b) represents the photothermal efficiency of our developed Fe_3O_4@C-PVPS and Fe_3O_4@C-PVPS:PEDOT nanoparticles (808 nm, 2 W/cm^2, 5 min).[18] Pure water was utilized as a control, for which virtually no temperature change was observed, whereas C-PVPS, Fe_3O_4@C-PVPS, and Fe_3O_4@C-PVPS:PEDOT (1:10 and 1:100) showed sharply raised thermal heat from 25 to 42 °C after 5 min of NIR irradiation, which was relatively higher at the 1/100 ratio of PEDOT than at the 1/10 composition ratio in the Fe_3O_4@C-PVPS nanoparticles. The photothermal conversion efficiencies (η) of free Fe_3O_4 and Fe_3O_4@C-PVPS:PEDOT (1:100) were calculated based on the energy balance of the system.[19,20] The η values of Fe_3O_4 and Fe_3O_4@C-PVPS:PEDOT (1:100) in water were found to be 24.58% and 51.14%, respectively (Figure S3, SI).[19,20] Based on the absorption peaks, the molar extinction coefficients (ε_{808}) of Fe_3O_4 and Fe_3O_4@CPVPS:PEDOT at 808 nm were found to be 2.31×10^3 and 3.27×10^3 M^{-1} cm^{-1}, respectively.[21] These results indicate that the Fe_3O_4@CPVPS:PEDOT photothermal conversions were related to NIR absorption whereas the free Fe_3O_4 photothermal conversions were not efficient compared with the pronounced NIR absorption. Additionally, the concentration-dependent photothermal elevation studies also supported the above scenario (Figure1c).

To characterize the material composition, X-ray photoelectron spectroscopy (XPS) measurements demonstrated the elemental and structural identity of Fe_3O_4@C-PVPS:PEDOT.[22] The survey scan of Fe_3O_4@C-PVPS coated with PEDOT showed main peaks of S 2p, C 1s, N 1s, and O 1s centered at 165, 284, 400, and 533 eV, respectively (Figure 2a). The C 1s core-level spectrum of C-PVPS-coated Fe_3O_4 was curve-fitted with three peak components with binding energies of about 284.6, 285.7, and 287.6 eV attributable to C—C, C—N, and C═O species, respectively, ensuring polymer encapsulation (Figure 2b). The nitrogen core-line spectrum revealed two components at 399 and 402 eV that are characteristic of neutral amine (N^0) and cationic amine (N^+) functions, respectively, and confirmed the quaternization of catechol with polymer PVP (Figure 2c). Moreover, the S 2p peak at 168 eV

DOI: 10.1021/acsami.5b02737
ACS Appl. Mater. Interfaces 2015, 7, 9469−9478

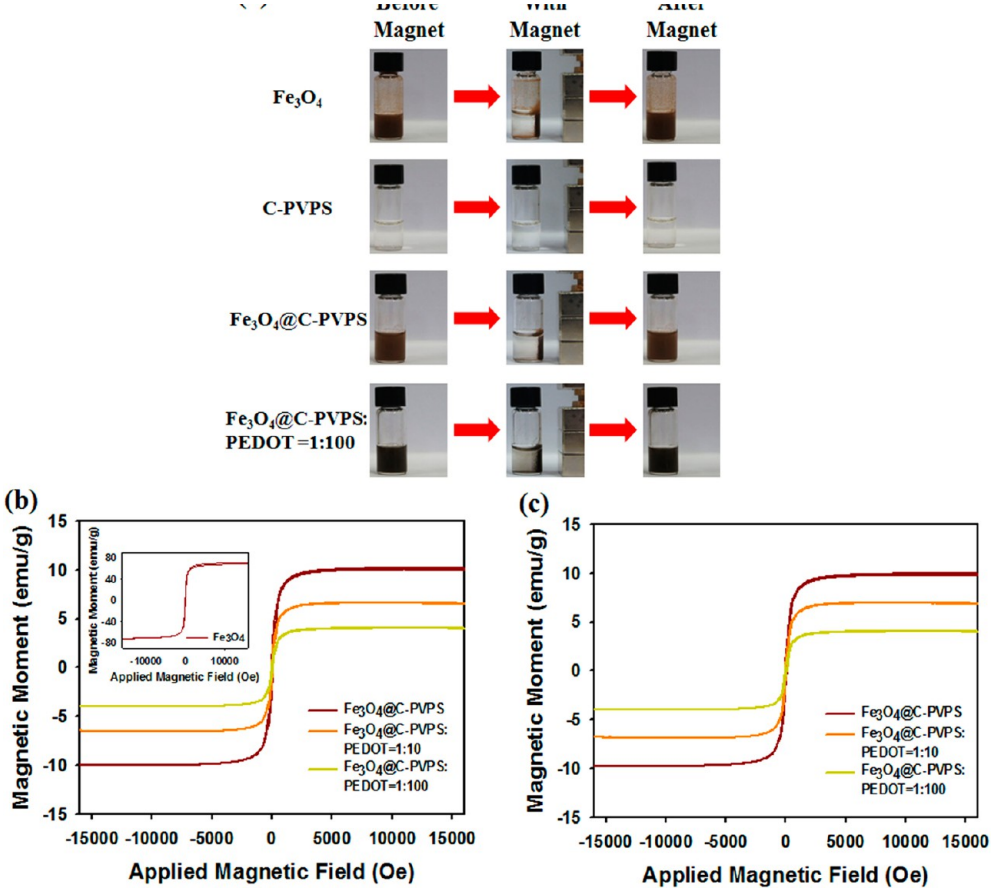

Figure 4. (a) Photographs of suspensions of Fe_3O_4, C-PVPS, Fe_3O_4@C-PVPS, and Fe_3O_4@C-PVPS:PEDOT (1:100) dispersed in water (left) before, (middle) while, and (right) after being placed around a magnet. (b) Field-dependent magnetization curves of Fe_3O_4@C-PVPS and Fe_3O_4@C-PVPS:PEDOT (1:100) at room temperature. Inset: Free Fe_3O_4 magnetization curve. (c) After NIR irradiation, the field-dependent magnetization curve of Fe_3O_4@C-PVPS, Fe_3O_4@C-PVPS:PEDOT (1:100) at room temperature. The laser wavelength was 808 nm, and the exposure time was 5 min at a power of 2 W/cm^2.

demonstrated the presence of SO_3^- groups due to the 3,4-ethylenedioxythiophene (EDOT) assembled around the fabricated Fe_3O_4 nanoparticles (Figure 2d).

Along with the evaluation of the elemental composition, the functionalized Fe_3O_4 with PEDOT was ascertained by transmission electron microscopy (TEM) imaging.[23,24] The TEM micrograph showed a thin structure around the Fe_3O_4@C-PVPS nanoparticles, and the outer thin layer became dense when the PEDOT was additionally cap assembled around the Fe_3O_4@C-PVPS nanoparticles (Figure 3). In dynamic light scattering (DLS) measurements, the average diameters of Fe_3O_4@C-PVPS:PEDOT (1:10) and Fe_3O_4@C-PVPS:PEDOT (1:100) were found to be 41.7 and 48.3 nm, respectively (Figure S4, SI). At the same time, the stability evaluated after 0 and 5 days, showing well-dispersed and suspended polymer-coated iron oxide nanoparticles where free iron oxide particles aggregated with time, resulting in lower NIR absorption (Figures S1 and S2, SI). The percentage of C-PVPS:PEDOT on the surface of the Fe_3O_4 was calculated by TGA measurements, giving 12% and 58% for the incorporated ratios of 1:10 and 1:100, respectively (Figure S5, SI). Moreover, the SEM images and EDX spectra also indicated an elevated level of polymer (C-PVPS) and PEDOT around the Fe_3O_4 nanoparticles for the C-PVPS:PEDOT composition (Figure S6, SI).

Nano-sized magnetic particles do not have a magnetic memory, but when a magnetic field is applied to the nanoparticles, a magnetic dipole is induced, and as soon as the external stimulus is removed, the particles return to their previous state. This reversible behavior of nano-sized magnetic particles helps to control the motion from externally applied magnetic fields.[25−27] With exposure to an external magnetic field, all Fe_3O_4, Fe_3O_4@C-PVPS, and Fe_3O_4@C-PVPS:PEDOT nanoparticles were attracted to the magnetic side, leaving the remaining solution completely colorless (Figure 4b). After the magnet was removed, the nanoparticles were readily dispersed in the aqueous solution. In field-dependent magnetization measurements, the Fe_3O_4@C-PVPS:PEDOT displayed strong magnetic properties, indicating a superparamagnetic nature, as shown in Figure 4a.[5,6] At the same time, the paramagnetic nature of the inner core of Fe_3O_4 was not significantly affected by NIR-irradiated photothermal heating (Figure 4c). Furthermore, the zeta potential analysis of Fe_3O_4@C-PVPS showed a reduced charge from positive to negative depending on the pH change from 5 to 9. This result is attributed to the negatively charged sultone group encapsulated on the neutral charged Fe_3O_4 nanoparticles.[22] However, when the EDOT assembled over the Fe_3O_4@C-PVPS particle surface, the charge potentiality exhibited a pH-dependent behavior, and at a higher ratio of EDOT (100), making colloidal stability, the material had an electrical potential of +10 mV at pH 5. The increased

DOI: 10.1021/acsami.5b02737
ACS Appl. Mater. Interfaces 2015, 7, 9469−9478

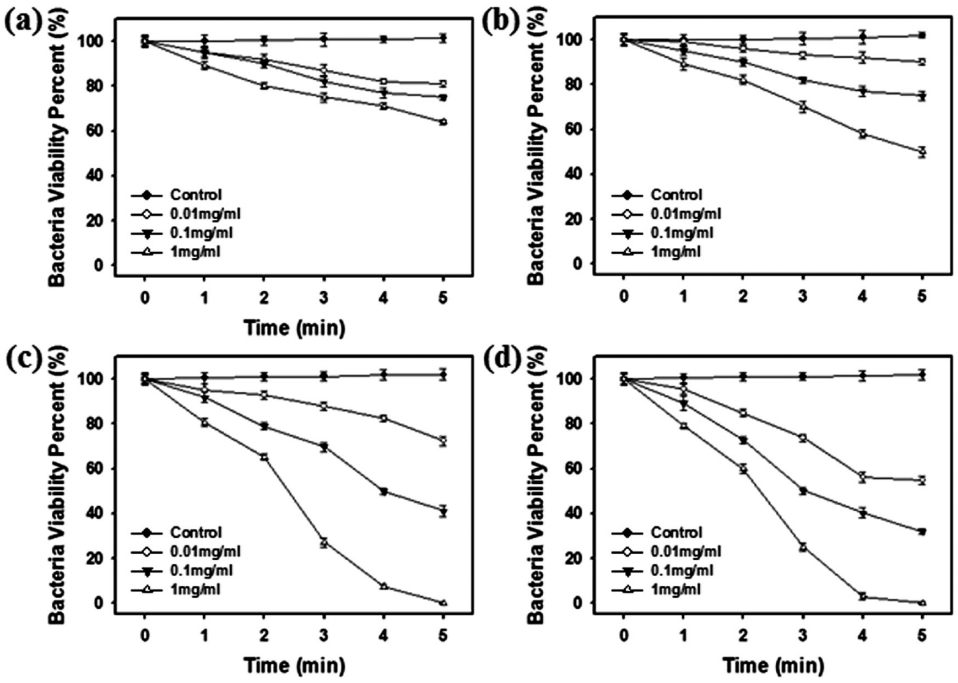

Figure 5. Photothermal effects of bacterial viability after treatment with (a,b) Fe_3O_4 and (c,d) Fe_3O_4@C-PVPS:PEDOT (1:100) under 808-nm laser irradiation for different times against (a,c) *S. aureus* and (b,d) *E. coli*. The laser power density was 2 W/cm^2.

positive potential also complies with the electrically positive potential of EDOT (3,4-ethylenedioxythiophene) on the Fe_3O_4@C-PVPS particle surface (Figure S7, SI).[22]

To test the effect of photothermal treatment, *S. aureus* (Gram-positive) and *E. coli* (Gram-negative) were first incubated with Fe_3O_4 and Fe_3O_4@C-PVPS:PEDOT for 30 min. NIR (808-nm) light was then used to irradiate the *S. aureus* and *E. coli* culture plates. After irradiation, an external magnetic field was used to isolate the treated sample (Fe_3O_4 and Fe_3O_4@C-PVPS:PEDOT) from the bacterial culture medium. The photothermal killing effect of bacteria was confirmed after 24 h by colony counting on the agar plates. It was found that the bacterial killing efficiency depended on both the NIR irradiation time and concentration, which differed for the Fe_3O_4- to Fe_3O_4@C-PVPS:PEDOT-treated agents. Figure 5 shows the bacteria killing percentages after 0, 1, 2, 3, 4, and 5 min of NIR exposure, where the killing efficiency increased with irradiation time and sample concentration. However, the Fe_3O_4@C-PVPS:PEDOT-treated agent exhibited a prominent antibacterial efficiency compared with its precursor Fe_3O_4. After 5 min of NIR treatment at a 1 mg/mL concentration, almost 100% of the bacteria were killed in the Fe_3O_4@C-PVPS:PEDOT-treated group (Figure 5c,d), whereas the Fe_3O_4-treated group showed a 55−60% killing efficiency under the same experimental condition (Figure 5a,b). The weak photothermal conversion and oxidative stress generated by free iron oxide shows a mild native toxicity to reduce bacterial viability.[28] However, the strong absorption of Fe_3O_4@C-PVPS:PEDOT at the irradiated wavelength resulted in photothermal activation that was converted to heat.[18] As a result, the strong activation released efficient thermal heat to induce irreversible bacterial destruction by photothermolysis. Moreover, the agent containing 1 mg of Fe_3O_4@C-PVPS:PEDOT performed 100% killing in a very short period of time for both bacterial strains. The temperature elevation dictated rapid photothermal killing of bacteria of both Gram-positive and Gram-negative strains. However, in the absence of NIR exposure, the bacterial viability remained almost unchanged under the same conditions (Figure S8, SI).

The recyclable antibacterial activity of Fe_3O_4@C-PVPS:PEDOT was examined against Gram-positive *S. aureus* and Gram-negative *E. coli* bacteria using the spread plate method.[29] Figure 6 shows that the bacterial killing efficiency depends strongly on the polymer composite around the iron oxide nanoparticles. The released heat propagated the thermolysis of the susceptible bacterial strain around this nanocomposite. The resulting thermolysis showed strain independence of 60% more killing potentiality than the free iron oxide nanoparticles (Figure 6).[30] Moreover, when the Fe_3O_4@C-PVPS:PEDOT was used multiple times by being recycled more than three times, the antibacterial efficiency was almost unchanged. The growing interest in developing recyclable antibacterial nanomaterials will therefore include the future perspective of Fe_3O_4@C-PVPS:PEDOT nanoparticles. To further demonstrate the NIR-irradiated photothermal antibacterial activity of Fe_3O_4@C-PVPS:PEDOT nanoparticles, we carried out a fluorescence-based cell viability assay to verify the bacteria survival rate. SYTO 9 for live cells and propidium iodide (PI) for dead bacterial cells labeled as fluorescent were used here to distinguish between live and dead bacteria.[31] As can be seen in Figure 7a, all bacteria (*S. aureus* and *E. coli*) were destroyed after being incubated with Fe_3O_4@C-PVPS:PEDOT nanoparticles and after exposure to 808-nm laser light at a power density of 2 W/cm^2, whereas the control group without the incubated nanoparticles did not shown any NIR-mediated antibacterial effect. Furthermore, nanoparticle uptake by the bacteria was demonstrated through 4,4-difluoro-1,3,5,7-tetramethyl-4-bora-3a,4a-diaza-*s*-indacene- (BODIPY-) labeled Fe_3O_4@C-PVPS:PEDOT, where green-colored dots indicate the presence of treated photothermal agents. However, the NIR-irradiated photothermal heat destroyed the cell viability, and application of a magnetic field can isolate the Fe_3O_4@C-

DOI: 10.1021/acsami.5b02737
ACS Appl. Mater. Interfaces 2015, 7, 9469−9478

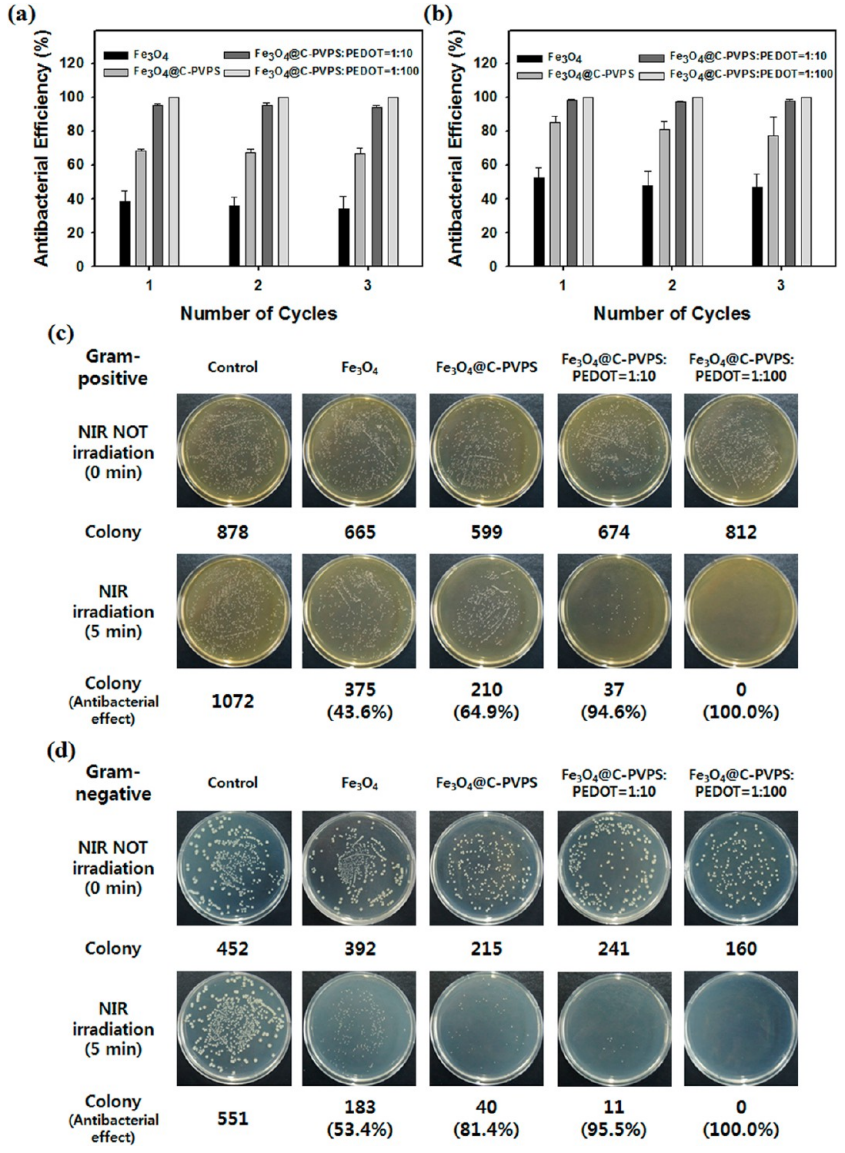

Figure 6. (a,b) Antibacterial efficiencies of continuous three-times-recycled Fe_3O_4@C-PVPS:PEDOT (1:100) (1 mg/mL) under 808-nm laser irradiation taken at 5 min against (a) *S. aureus* and (b) *E. coli*. (c,d) Photographic images of the numbers of colonies of zone inhibition of (c) Gram-positive (*S. aureus*) and (d) Gram-negative (*E. coli*) bacteria after 5 min of NIR irradiation and overnight incubation for different treated samples of Fe_3O_4, Fe_3O_4@C-PVPS, and Fe_3O_4@C-PVPS:PEDOT (1:10 and 1:100). The control group was treated with only NIR irradiation. The laser power density was 2 W/cm^2.

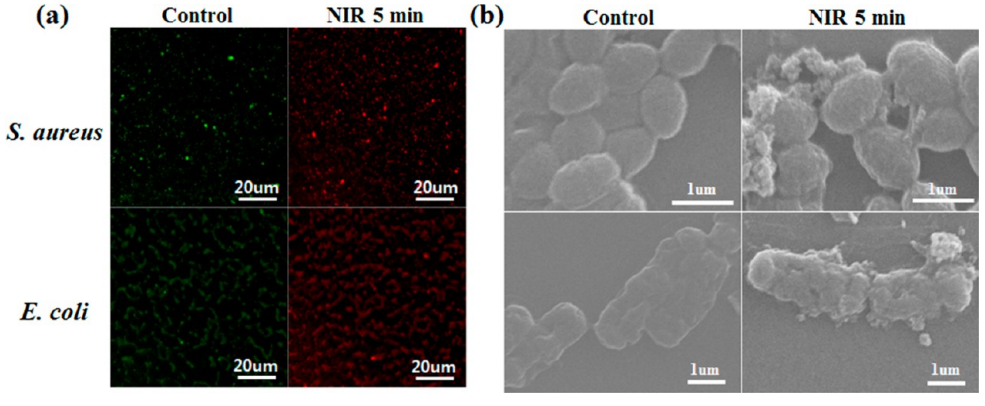

Figure 7. (a) Fluorescence microscopy images showing the PTT cytotoxicity of *S. aureus* and *E. coli* after 5 min of 808-nm NIR irradiation with Fe_3O_4@C-PVPS:PEDOT (1:100) in SYTO 9 and PI (scale = 20 μm). (b) Scanning electron microscopy (SEM) images of (top) *S. aureus* and (bottom) *E. coli* after 5 min of 808-nm NIR irradiation with Fe_3O_4@C-PVPS:PEDOT (1:100). The laser power density was 2 W/cm^2.

DOI: 10.1021/acsami.5b02737
ACS Appl. Mater. Interfaces 2015, 7, 9469−9478

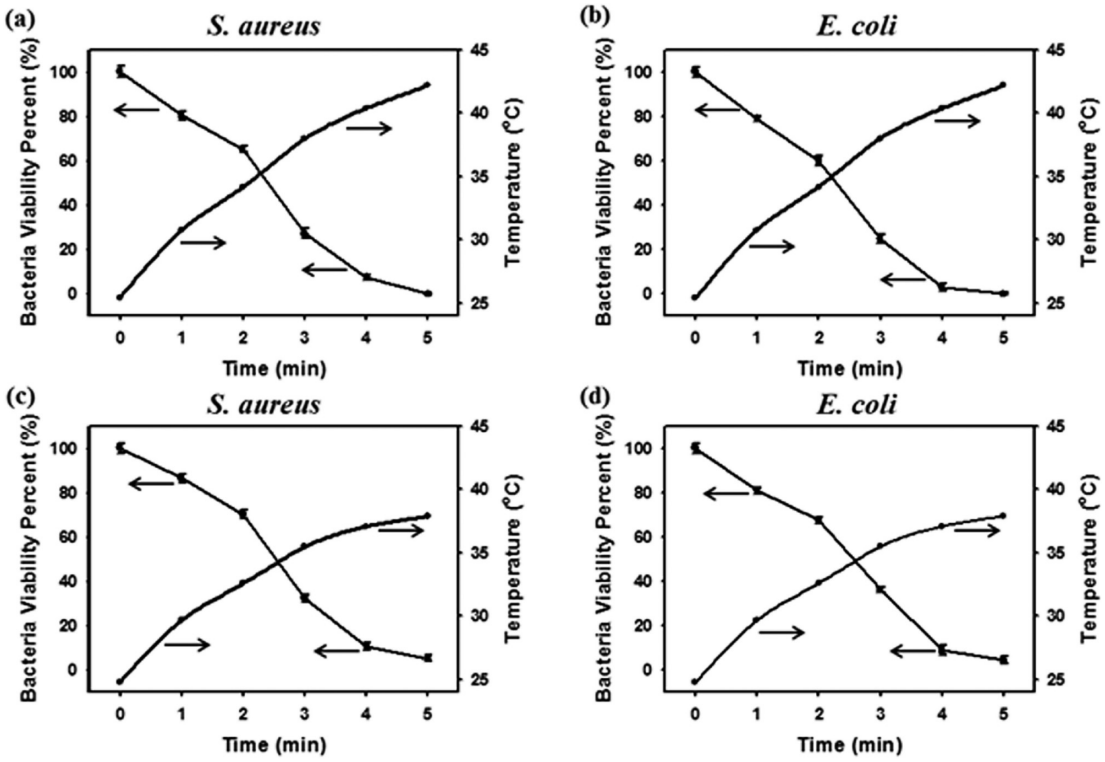

Figure 8. Temperature- and time- (NIR irradiation) dependent percentages of bacterial viability upon treatment with (a,b) Fe_3O_4@C-PVPS:PEDOT (1:100) and (c,d) Fe_3O_4@C-PVPS:PEDOT (1:10) for (a,c) *S. aureus* and (b,d) *E. coli* bacteria.

PVPS:PEDOT nanoparticles by breaking the cell membrane (Figure S9, SI).[32] At the same time, SEM images were taken to evaluate the morphologies of both native and fabricated iron oxide nanoparticles with PTT polymer (Figure 7b). The control *S. aureus* and *E. coli* retained undamaged structures. However, Fe_3O_4@C-PVPS:PEDOT-treated bacteria exhibited a destroyed surface with a groove-like structure.[33,34] Therefore, the time- (NIR irradiation) and temperature-dependent percentage of bacterial viability demonstrated reasonable photothermal effects that were also ascribed the above-observed results (Figure 8 and Figure S10, SI). The rapid killing efficiency of Fe_3O_4@C-PVPS:PEDOT nanoparticles toward both bacterial strains demonstrates the photothermal conversion efficiency of the photothermal antibacterial agent.

CONCLUSIONS

We functionalized Fe_3O_4 nanoparticles with catechol/sultone-conjugated PVP that was subsequently encapsulated with PEDOT to develop NIR-irradiated photothermal antibacterial nanoparticles. Our developed antibacterial agent shows sufficient photothermal heat efficiency for killing bacteria against both Gram-positive and Gram-negative strains in a very short period of time. We also demonstrated that Fe_3O_4@C-PVPS:PEDOT antibacterial nanoparticles can be recycled, allowing for multiple applications. XPS-, TEM-, and SEM-based structural and morphological character analysis with magnetic property evaluation revealed promising advantages. Furthermore, NIR-irradiated efficient thermal heat generation performed similarly to nanoscopic heaters, enabling the use of recyclable antibacterial magnetic nanoparticles. Although the study of this area is still in its early stages, properly chosen combinations and continued development of nanomaterial-based antibacterial agents are very important for advancing this exciting and rapidly changing field.

ASSOCIATED CONTENT

Supporting Information

Additional information as noted in text. The Supporting Information is available free of charge on the ACS Publications website at DOI: 10.1021/acsami.5b02737.

AUTHOR INFORMATION

Corresponding Authors

*E-mail: in1@cjnu.ac.kr (I.I.).
*E-mail: parkchem@ut.ac.kr (S.Y.P.).

Notes

The authors declare no competing financial interest.

ACKNOWLEDGMENTS

This work was supported by Grants 10046506 and 10048377 from the Ministry of Trade, Industry and Energy (MOTIE) and was also by the Basic Science Research Program through the National Research Foundation of Korea (NRF) funded by the Ministry of Education (No. 2014055946).

REFERENCES

(1) *The Evolving Threat of Antimicrobial Resistance: Options for Action*; World Health Organization: Geneva, Switzerland, 2012.
(2) Huang, W. C.; Tsai, P. J.; Chen, Y. C. Multifunctional Fe_3O_4@Au Nanoeggs as Photothermal Agents for Selective Killing of Nosocomial and Antibiotic-Resistant Bacteria. *Small* **2009**, *5*, 51−56.
(3) Stevanović, M.; Uskoković, V.; Filipović, M.; Škapin, S. D.; Uskoković, D. Composite PLGA/AgNpPGA/AscH Nanospheres with Combined Osteoinductive, Antioxidative, and Antimicrobial Activities. *ACS Appl. Mater. Interfaces* **2013**, *5*, 9034−9042.

DOI: 10.1021/acsami.5b02737
ACS Appl. Mater. Interfaces 2015, 7, 9469−9478

(4) Hajipour, M. J.; Fromm, K. M.; Ashkarran, A. A.; de Aberasturi, D. J.; de Larramendi, I. R.; Rojo, T.; Serpooshan, V.; Parak, W. J.; Mahmoudi, M. Antibacterial Properties of Nanoparticles. *Trends Biotechnol.* **2012**, *30*, 499−511.
(5) Liu, J.; Zhao, Z.; Feng, H.; Cui, F. One-Pot Synthesis of Ag−Fe_3O_4 Nanocomposites in the Absence of Additional Reductant and Its Potent Antibacterial Properties. *J. Mater. Chem.* **2012**, *22*, 13891−13894.
(6) Santhosh, C.; Kollu, P.; Doshi, S.; Sharma, M.; Bahadur, D.; Vanchinathan, M. T.; Saravanan, P.; Kime, B. S.; Grace, A. N. Adsorption, Photodegradation and Antibacterial Study of Graphene−Fe_3O_4 Nanocomposite for Multipurpose Water Purification Application. *RSC Adv.* **2014**, *4*, 28300−28308.
(7) Liu, L.; Liu, J.; Wang, Y.; Yan, X.; Sun, D. D. Facile Synthesis of Monodispersed Silver Nanoparticles on Graphene Oxide Sheets with Enhanced Antibacterial Activity. *New J. Chem.* **2011**, *35*, 1418−1423.
(8) Dong, H.; Huang, J.; Koepsel, R. R.; Ye, P.; Russell, A. J.; Matyjaszewski, K. Recyclable Antibacterial Magnetic Nanoparticles Grafted with Quaternized Poly(2-(dimethylamino)ethyl methacrylate) Brushes. *Biomacromolecules* **2011**, *12*, 1305−1311.
(9) Cai, X.; Lin, M.; Tan, S.; Mai, W.; Zhang, Y.; Liang, Z.; Lin, Z.; Zhang, X. The Use of Polyethyleneimine-Modified Reduced Graphene Oxide as a Substrate for Silver Nanoparticles to Produce a Material with Lower Cytotoxicity and Long-Term Antibacterial Activity. *Carbon* **2012**, *50*, 3407−3415.
(10) Zhao, Y.; Tian, Y.; Cui, Y.; Liu, W.; Ma, W.; Jiang, X. Small Molecule-Capped Gold Nanoparticles as Potent Antibacterial Agents That Target Gram-Negative Bacteria. *J. Am. Chem. Soc.* **2010**, *132*, 12349−12356.
(11) Xiong, Y.; Washio, I.; Chen, J.; Cai, H.; Li, Z. Y.; Xia, Y. Poly(vinyl pyrrolidone): A Dual Functional Reductant and Stabilizer for the Facile Synthesis of Noble Metal Nanoplates in Aqueous Solutions. *Langmuir* **2006**, *22*, 8563−8570.
(12) Shi, X.; Gong, H.; Li, Y.; Wang, C.; Cheng, L.; Liu, Z. Graphene-Based Magnetic Plasmonic Nanocomposite for Dual Bioimaging and Photothermal Therapy. *Biomaterials* **2013**, *34*, 4786−4793.
(13) Groenendaal, L.; Jonas, F.; Freitag, D.; Pielartzik, H.; Reynolds, J. R. Poly(3,4-ethylenedioxythiophene) and Its Derivatives: Past, Present, and Future. *Adv. Mater.* **2000**, *12*, 481−494.
(14) Han, M. G.; Foulger, S. H. Preparation of Poly(3,4-ethylenedioxythiophene) (PEDOT) Coated Silica Core−Shell Particles and PEDOT Hollow Particles. *Chem. Commun.* **2004**, 2154−2155.
(15) Song, X.; Chen, Q.; Liu, Z. Recent Advances in the Development of Organic Photothermal Nano-agents. *Nano Res.* **2015**, *8*, 340−354.
(16) Mosaiab, T.; Jeong, C. J.; Shin, G.; Choi, K. H.; Lee, S. K.; Lee, I.; In, I.; Park, S. Y. Recyclable and Stable Silver Deposited Magnetic Nanoparticles with Poly(vinyl pyrrolidone)-Catechol Coated Iron Oxide for Antimicrobial Activity. *Mater. Sci. Eng., C* **2013**, *33*, 3786−3794.
(17) Lee, S. Y.; Kim, S. H.; Kim, S. M.; Lee, H.; Lee, G.; Park, S. Y. Tunable and Selective Detection of Cancer Cells Using a Betainized Zwitterionic Polymer with BODIPY and Graphene Oxide. *New J. Chem.* **2014**, *38*, 2225−2228.
(18) Cheng, L.; Yang, K.; Chen, Q.; Liu, Z. Organic Stealth Nanoparticles for Highly Effective in Vivo Near-Infrared Photothermal Therapy of Cancer. *ACS Nano* **2012**, *6*, 5605−5613.
(19) Mebrouk, K.; Chotard, F.; Goff-Gaillard, C. L.; Arlot-Bonnemains, Y.; Fourmigué, M.; Camerel, F. Water-Soluble Nickel-bis(dithiolene) Complexes as Photothermal Agents. *Chem. Commun.* **2015**, *51*, 5268−5270.
(20) Liu, Y.; Ai, K.; Liu, J.; Deng, M.; He, Y.; Lu, L. Dopamine-Melanin Colloidal Nanospheres: An Efficient Near-Infrared Photothermal Therapeutic Agent for in Vivo Cancer Therapy. *Adv. Mater.* **2013**, *25*, 1353−1359.
(21) Zhou, T.; Wu, B.; Xing, D. Bio-modified Fe_3O_4 Core/Au Shell Nanoparticles for Targeting and Multimodal Imaging of Cancer Cell. *J. Mater. Chem.* **2012**, *22*, 470−477.
(22) Ouyang, J.; Xu, Q.; Chu, C. W.; Yang, Y.; Li, G.; Shinar, J. On the Mechanism of Conductivity Enhancement in Poly(3,4-ethylenedioxythiophene):Poly(styrene sulfonate) Film through Solvent Treatment. *Polymer* **2004**, *45*, 8443−8450.
(23) Kong, H.; Song, J.; Jang, J. One-Step Fabrication of Magnetic γ-Fe_2O_3/Polyrhodanine Nanoparticles Using *in Situ* Chemical Oxidation Polymerization and Their Antibacterial Properties. *Chem. Commun.* **2010**, *46*, 6735−6737.
(24) Kirchmeyer, S.; Reuter, K. Scientific Importance, Properties and Growing Applications of Poly(3,4-ethylenedioxythiophene). *J. Mater. Chem.* **2005**, *15*, 2077−2088.
(25) Mao, H.; Lu, X.; Liu, X.; Tang, J.; Wang, C.; Zhang, W. Preparation and Characterization of PEDOT/β-$Fe^{3+}O$(OH,Cl) Nanospindles with Controllable Sizes in Aqueous Solution. *J. Phys. Chem. C* **2009**, *113*, 9465−9472.
(26) Wang, C.; Xu, H.; Liang, C.; Liu, Y.; Li, Z.; Yang, G.; Cheng, L.; Li, Y.; Liu, Z. Iron Oxide @ Polypyrrole Nanoparticles as a Multifunctional Drug Carrier for Remotely Controlled Cancer Therapy with Synergistic Antitumor Effect. *ACS Nano* **2013**, *7*, 6782−6795.
(27) Song, X.; Gong, H.; Yin, S.; Cheng, L.; Wang, C.; Li, Z.; Li, Y.; Wang, X.; Liu, G.; Liu, Z. Ultra-Small Iron Oxide Doped Polypyrrole Nanoparticles for in Vivo Multimodal Imaging Guided Photothermal Therapy. *Adv. Funct. Mater.* **2014**, *24*, 1194−1201.
(28) Touati, D. Iron and Oxidative Stress in Bacteria. *Arch. Biochem. Biophys.* **2000**, *373*, 1−6.
(29) Yang, S.; Zong, P.; Ren, X.; Wang, Q.; Wang, X. Rapid and Highly Efficient Preconcentration of Eu(III) by Core−Shell Structured Fe_3O_4@Humic Acid Magnetic Nanoparticles. *ACS Appl. Mater. Interfaces* **2012**, *4*, 6891−6900.
(30) Hsiao, C.-W.; Chen, H.-L.; Liao, Z.-X.; Sureshbabu, R.; Hsiao, H.-C.; Lin, S.-J.; Chang, Y.; Sung, H.-W. Effective Photothermal Killing of Pathogenic Bacteria by Using Spatially Tunable Colloidal Gels with Nano-Localized Heating Sources. *Adv. Funct. Mater.* **2014**, *25*, 721−728.
(31) Ghosh, C.; Manjunath, G. B.; Akkapeddi, P.; Yarlagadda, V.; Hoque, J.; Uppu, D. S. S. M.; Konai, M. M.; Haldar, J. Small Molecular Antibacterial Peptoid Mimics: The Simpler the Better! *J. Med. Chem.* **2014**, *57*, 1428−1436.
(32) Ramasamy, M.; Lee, S. S.; Kee, D.; Kim, K. Magnetic, Optical Gold Nanorods for Recyclable Photothermal Ablation of Bacteria. *J. Mater. Chem. B* **2014**, *2*, 981−988.
(33) Ballav, N.; Choi, H. J.; Mishra, S. B.; Maity, A. Synthesis, Characterization of Fe_3O_4@glycine Doped Polypyrrole Magnetic Nanocomposites and Their Potential Performance to Remove Toxic Cr(VI). *J. Ind. Eng. Chem.* **2014**, *20*, 4085−4093.
(34) Santhosh, C.; Kollu, P.; Doshi, S.; Sharma, M.; Bahadur, D.; Vanchinathan, M. T.; Saravanan, P.; Kim, B. S.; Grace, A. N. Adsorption, Photodegradation and Antibacterial Study of Graphene−Fe_3O_4 Nanocomposite for Multipurpose Water Purification Application. *RSC Adv.* **2014**, *4*, 28300−28308.

DOI: 10.1021/acsami.5b02737
ACS Appl. Mater. Interfaces 2015, 7, 9469−9478